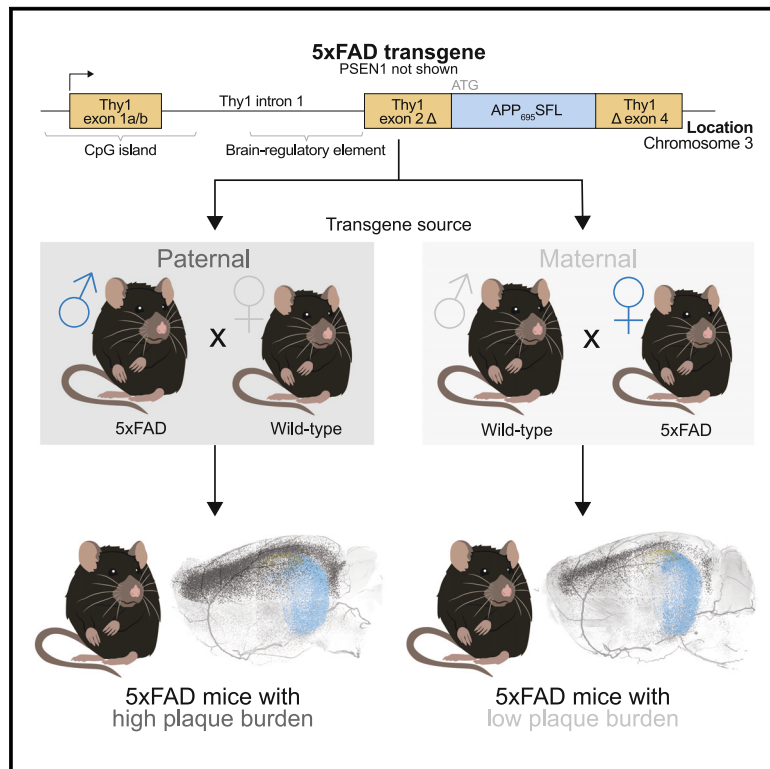


# Parental origin of transgene modulates amyloid- $\beta$ plaque burden in the 5xFAD mouse model of Alzheimer's disease

## Graphical abstract



## Authors

Andrew Octavian Sasmita,  
Erinne Cherisse Ong,  
Taisiia Nazarenko, ..., Beth Stevens,  
Constanze Depp, Klaus-Armin Nave

## Correspondence

sasmita@mpinat.mpg.de (A.O.S.),  
depp@broadinstitute.org (C.D.),  
nave@mpinat.mpg.de (K.-A.N.)

## In brief

The 5xFAD transgenic model, popular in Alzheimer's disease research, exhibits varying cerebral plaque burden depending on the parental source of the transgene. Mice inheriting the transgene paternally showed twice the amyloid plaque amount found in mice with a maternal inheritance, emphasizing the need to report detailed breeding schemes in studies.

## Highlights

- Mice inheriting the 5xFAD transgene paternally develop higher amyloid plaque burden
- This transgenic inheritance effect is independent of mouse age, sex, and colony
- Maternal inheritance lowers Thy1.2-driven transgene expression, suggesting imprinting
- 5xFAD studies could potentially be confounded by this inheritance effect



Report

# Parental origin of transgene modulates amyloid- $\beta$ plaque burden in the 5xFAD mouse model of Alzheimer's disease

Andrew Octavian Sasmita,<sup>1,2,\*</sup> Erinne Cherisse Ong,<sup>1,2</sup> Taisiia Nazarenko,<sup>1,2,3,4</sup> Shuying Mao,<sup>1</sup> Lina Komarek,<sup>1</sup> Maik Thalmann,<sup>5</sup> Veronika Hantakova,<sup>1</sup> Lena Spieth,<sup>3,4</sup> Stefan A. Berghoff,<sup>3,4</sup> Helena J. Barr,<sup>7</sup> Maximilian Hingerl,<sup>7,8</sup> Friederike Börensens,<sup>1</sup> Johannes Hirrlinger,<sup>1,6</sup> Mikael Simons,<sup>3,4,9,10</sup> Beth Stevens,<sup>7,8,11</sup> Constanze Depp,<sup>1,7,8,12,\*</sup> and Klaus-Armin Nave<sup>1,\*</sup>

<sup>1</sup>Department of Neurogenetics, Max Planck Institute for Multidisciplinary Sciences, Göttingen, Germany

<sup>2</sup>International Max Planck Research School for Neurosciences, Göttingen, Germany

<sup>3</sup>Institute of Neuronal Cell Biology, Technical University Munich, Munich, Germany

<sup>4</sup>German Center for Neurodegenerative Diseases (DZNE), Munich, Germany

<sup>5</sup>Department of English Philology, Georg-August University, Göttingen, Germany

<sup>6</sup>Carl-Ludwig-Institute for Physiology, Faculty of Medicine, University of Leipzig, Leipzig, Germany

<sup>7</sup>F.M. Kirby Neurobiology Center, Department of Neurology, Boston Children's Hospital, Harvard Medical School, Boston, MA, USA

<sup>8</sup>Stanley Center for Psychiatric Research, Broad Institute of MIT and Harvard, Cambridge, MA, USA

<sup>9</sup>Munich Cluster of Systems Neurology (SyNergy), Munich, Germany

<sup>10</sup>Institute for Stroke and Dementia Research, University Hospital of Munich, LMU Munich, Munich, Germany

<sup>11</sup>Howard Hughes Medical Institute, Boston Children's Hospital, Harvard Medical School, Boston, MA, USA

<sup>12</sup>Lead contact

\*Correspondence: [sasmita@mpinat.mpg.de](mailto:sasmita@mpinat.mpg.de) (A.O.S.), [depp@broadinstitute.org](mailto:depp@broadinstitute.org) (C.D.), [nave@mpinat.mpg.de](mailto:nave@mpinat.mpg.de) (K.-A.N.)

<https://doi.org/10.1016/j.neuron.2024.12.025>

## SUMMARY

In Alzheimer's disease (AD) research, the 5xFAD mouse model is commonly used as a heterozygote crossed with other genetic models to study AD pathology. We investigated whether the parental origin of the 5xFAD transgene affects plaque deposition. Using quantitative light-sheet microscopy, we found that paternal inheritance of the transgene led to a 2-fold higher plaque burden compared with maternal inheritance, a finding consistent across multiple 5xFAD colonies. This effect was not due to gestation or rearing by 5xFAD females. Immunoblotting suggested that transgenic inheritance modulates transgenic protein expression, potentially due to genomic imprinting of the Thy1.2 promoter. Surprisingly, fewer than 20% of 5xFAD studies report breeding schemes, suggesting that this factor might confound previous findings. Our data highlight a significant determinant of plaque burden in 5xFAD mice and underscore the importance of reporting the parental origin of the transgene to improve scientific rigor and reproducibility in AD research.

## INTRODUCTION

Published almost 20 years ago, the 5xFAD mouse model serves as a robust and widely used tool to study amyloidosis in Alzheimer's disease (AD) *in vivo*. To generate 5xFAD mice, the Vasar lab introduced two Thy 1.2-promoter-driven transgenes into the mouse genome: a human amyloid precursor protein (APP) transgene, bearing the Swedish, London, and Florida mutations that cause aggressive familial AD forms, and a human presenilin 1 (PSEN1) transgene harboring another two familial AD-linked mutations, M146L and L286V.<sup>1</sup> Notably, 5xFAD mice exhibit marked amyloid plaque deposition and reactive gliosis at a relatively young age, making them an attractive AD model for researchers.<sup>1</sup> However, this model comes with a set of limitations, including the non-endogenous expression levels of mutated APP

due to its transgenic nature.<sup>2</sup> Additionally, APP overexpression in this model only occurs in a subset of excitatory neurons wherein the Thy1.2 promoter is active, most notably neurons belonging to the hippocampal subiculum, cornu ammonis 1 (CA1), and cortical layer 5 regions.

A well-known yet incompletely understood feature of 5xFAD mice is their inherent variability in plaque deposition. The most common method to generate experimental 5xFAD mice is to breed a 5xFAD heterozygote with a non-5xFAD mouse. In this study, we asked whether the breeding scheme utilized to generate experimental cohorts (i.e., maternal or paternal inheritance of the transgene) can modulate plaque pathology in the offspring. Here, we focused on characterizing modulators of *in toto* plaque burden in congenic C57BL/6 5xFAD lines by quantitative light-sheet microscopy (LSM).



## RESULTS

### LSM as a powerful tool to unravel modulators of A $\beta$ pathology in 5xFAD mice

Classically, plaque pathology in AD mouse models is studied in histological brain sections. However, because only a few sections per mouse are stained, this technique can introduce technical variabilities and does not allow for visualization of plaque deposition across all brain regions at once. We previously established an LSM workflow to assess amyloid pathology *in toto* via Congo red labeling of plaques.<sup>3</sup> We first assessed whether this technique could unravel known primary modulators of plaque deposition in 5xFAD mice, namely age and sex. First, we aimed to characterize amyloid- $\beta$  (A $\beta$ ) plaque burden of male 5xFAD mice temporally from 3 to 14 months of age (Figure S1; Data S2). From each hemibrain, we analyzed the total number of plaques (Figure S1B), average individual plaque volume (Figure S1C), total plaque volume (Figure S1D), plaque density in 3D (Figure S1D), and volume of region of interest (Figure S1F). Using LSM, we showed that plaque burden in these mice progresses rapidly over the first few months, particularly from 3 to 8 months, after which increases in plaque number plateau (Figures S1B and S1E). Nevertheless, individual plaques still grow in volume at later ages (Figures S1C and S1D), which corroborates the sigmoidal growth kinetics of A $\beta$  plaques.<sup>4</sup> When testing the effects of experimental interventions such as drug treatments or genetic manipulations in 5xFAD mice, our data also suggest that early time points in the range of 3–6 months should be prioritized to target a window in which amyloid deposition is at its greatest dynamic range. Next, we investigated whether LSM can characterize the known sex dimorphism in 5xFAD mice.<sup>5–7</sup> For this, we compared 6-month-old male and female 5xFAD mice. Female 5xFAD mice developed approximately twice the plaque burden compared with their age-matched male counterparts (Figure S2), with the most striking difference in plaque load found in the cortex (Figures S2B–S2D). In summary, LSM of Congo red-labeled brains can be effectively used to study plaque modulation on a brain-wide scale.

### Parental origin of transgene influences plaque burden in 5xFAD mice

Next, we utilized LSM to study whether the transgenic inheritance pattern influences plaque burden in 5xFAD mice (Figure 1; Data S2). Breeding schemes to generate experimental cohorts of 5xFAD animals typically use a heterozygous 5xFAD breeder, where either the mother or father is transgene positive, crossed with non-5xFAD mice from a mouse strain of interest to generate crossbreeds or bred with wild-type (WT) controls for maintenance of pure 5xFAD lines. We assessed cohorts of male 5xFAD mice carrying transgenes inherited either paternally or maternally and analyzed their plaque burden at 6 months of age (Figure 1A). Interestingly, 5xFAD mice that acquired their transgene paternally developed significantly more plaques. This was most striking in the cortex, where a 2-fold difference was observed in comparison with mice with a maternal transgenic inheritance (Figures 1B and 1C). As plaques grow both in number and size, we also observed that plaques are smaller in

5xFAD mice with a maternal inheritance. These observed differences were accompanied by unchanged volumes of regions of interest, excluding the possibility that total changes in plaque pathology were mediated by changes in brain volume.

### Inheritance effect is mainly dictated by the parental source across generations

We then asked whether the grandparental pedigree of 5xFAD mice also influences plaque burden in the resulting offspring. Therefore, we assessed four groups: paternal-grandpaternal (PGP), paternal-grandmaternal (PGM), maternal-grandpaternal (MGP), and maternal-grandmaternal (MGM) (Figures S3A and S3B; Data S2). Mice inheriting the transgene via two consecutive maternal sources (MGM) exhibited a small yet additive dampening of cortical and hippocampal plaque numbers but no other analyzed parameters (Data S2). Nevertheless, the effect of the grandparental transgenic source is minimal, with the parental transgenic source masking the grandparental effect. This is seen in the plaque burden of PGM brains returning to PGP levels (Figure S3B). We conclude that the parental transgenic source ablates the grandparental influence almost completely and is the determining factor in plaque burden modulation by the proposed inheritance effect.

### Transgenic inheritance effect is universal in congenic C57BL/6 5xFAD mice

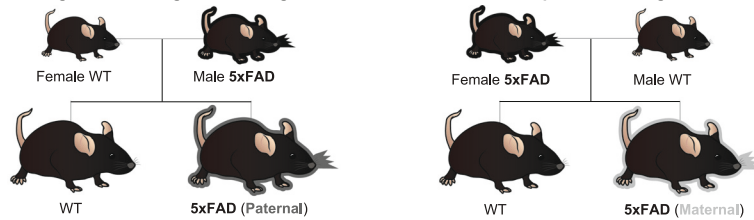
Next, we considered whether the transgenic inheritance effect had only been acquired in our local congenic 5xFAD strain or whether this was a universal effect in multiple congenic 5xFAD colonies. We therefore investigated plaque burden in two further 5xFAD substrains from different institutions: cohort B housed in another facility in Germany (Munich) and cohort C housed in an animal core in the United States (Boston). Of note, cohort C had been freshly derived from The Jackson Laboratory congenic stock and only underwent one breeding cycle with C57BL/6J mice at the local facility. Importantly, we could corroborate the observed inheritance effect in these animal cohorts (Figures 2A–2D; Data S2) in both sexes and at different ages. Due to a limited number of animals, we further supplemented our primary findings with a qualitative assessment of the same effect in male 5xFAD mice from cohort C (Figures S3C and S3D). Our findings indicate that the effect is present in the line directly derived from The Jackson Laboratory, from where most researchers acquire the 5xFAD mouse model. Furthermore, our findings highlight the universal nature of plaque burden modulation caused by distinct transgenic inheritance patterns in the congenic 5xFAD line.

### Inheritance effect is absent in heterozygous APP<sup>NLGF</sup> knockin mice

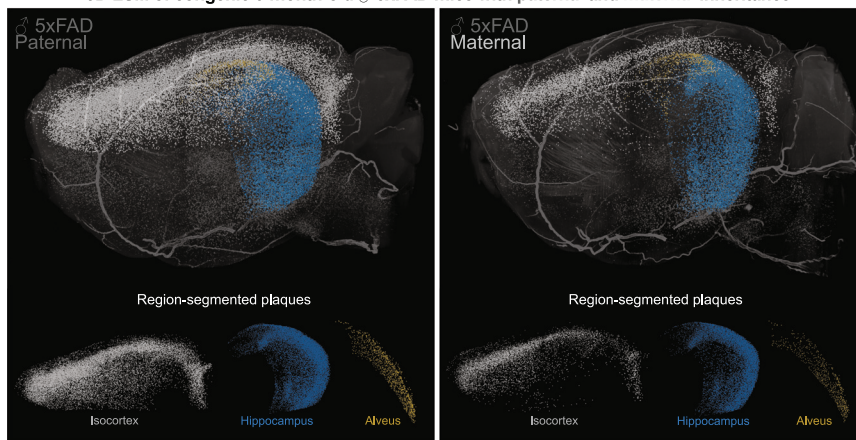
Although the 5xFAD mouse model is one of the most widely used to study amyloidosis in the context of AD, various others exist to simulate amyloidosis, including more recently developed knockin mouse models. Thus, we asked whether the observed effect is specific to 5xFAD mice or a more general feature of mouse models of AD. We aimed to determine whether the inheritance effect is present in a mouse model wherein the mutated APP version is driven by its endogenous promoter and not from a transgenic construct. For this, we turned to

### A Parental transgene source modulates plaque burden in 5xFAD offspring

Breeding schemes to generate congenic 5xFAD mice with different parental transgenic sources



### B 3D LSM of congenic 6-month-old ♂ 5xFAD mice with paternal and maternal inheritance



### C LSM data quantification of 6-month-old ♂ 5xFAD mice with paternal and maternal inheritance

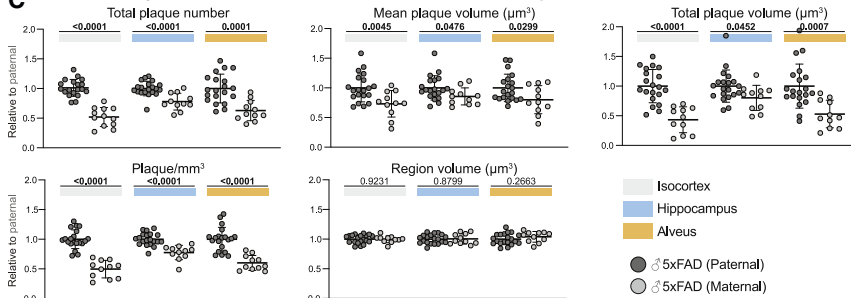


### Figure 1. 5xFAD animals with a paternal transgenic inheritance develop more plaques than their maternal counterparts

(A) Breeding schemes to generate 5xFAD animals with distinct parental transgenic sources.

(B) LSM 3D visualization of male 5xFAD hemibrains of animals with paternal and maternal inheritance at 6 months of age. Color-region allocation is as follows: white, isocortex; blue, hippocampus; and yellow, alveus.

(C) Quantification of male 5xFAD data with paternal ( $n = 20$ ) and maternal ( $n = 11$ ) inheritance. Maternal data points were normalized to paternal data. Dark gray shapes represent paternal data, and light gray shapes represent maternal data. For each parameter, an unpaired, two-tailed Student's  $t$  test was performed ( $p$  values indicated in graphs, significant  $p$  values [ $<0.05$ ] highlighted in bold) comparing paternal with maternal inheritance. Thick lines represent means with SD (thin lines) and individual data points displayed. Raw unnormalized data are available in [Data S2](#).

rendering the offspring more resilient to the pathology.<sup>8</sup> To test this, we set up breeder pairs, with both parents being heterozygous for the 5xFAD transgene (Figure S4A). In this breeding paradigm, heterozygous offspring could either inherit the 5xFAD transgene paternally or maternally while developing in a 5xFAD dam. If the maternal immune priming hypothesis holds true, then all sex-matched heterozygous offspring from this breeding scheme should develop similar plaque loads despite a proportion having inherited the transgene from the father. However, this was not the case, as some animals developed much higher plaque loads compared with others (Figures S4B–S4D). This bifurcated distribution of plaque burden in offspring of

heterozygous *APP<sup>NLGF</sup>* mice in which one allele of APP is humanized and mutated in its endogenous locus. Analysis of heterozygous *APP<sup>NLGF</sup>* mice with either *APP<sup>NLGF</sup>* mothers or fathers revealed that all offspring developed comparable plaque load (Figures 2E and 2F; [Data S2](#)). This indicates that the transgenic inheritance pattern only influences plaque burden when APP is driven by an exogenous promoter in a different genomic locus, which may point to the 5xFAD transgene construct or promoter undergoing genomic imprinting.

### Plaque burden modulation is not a result of gestation in or rearing by a 5xFAD-positive female

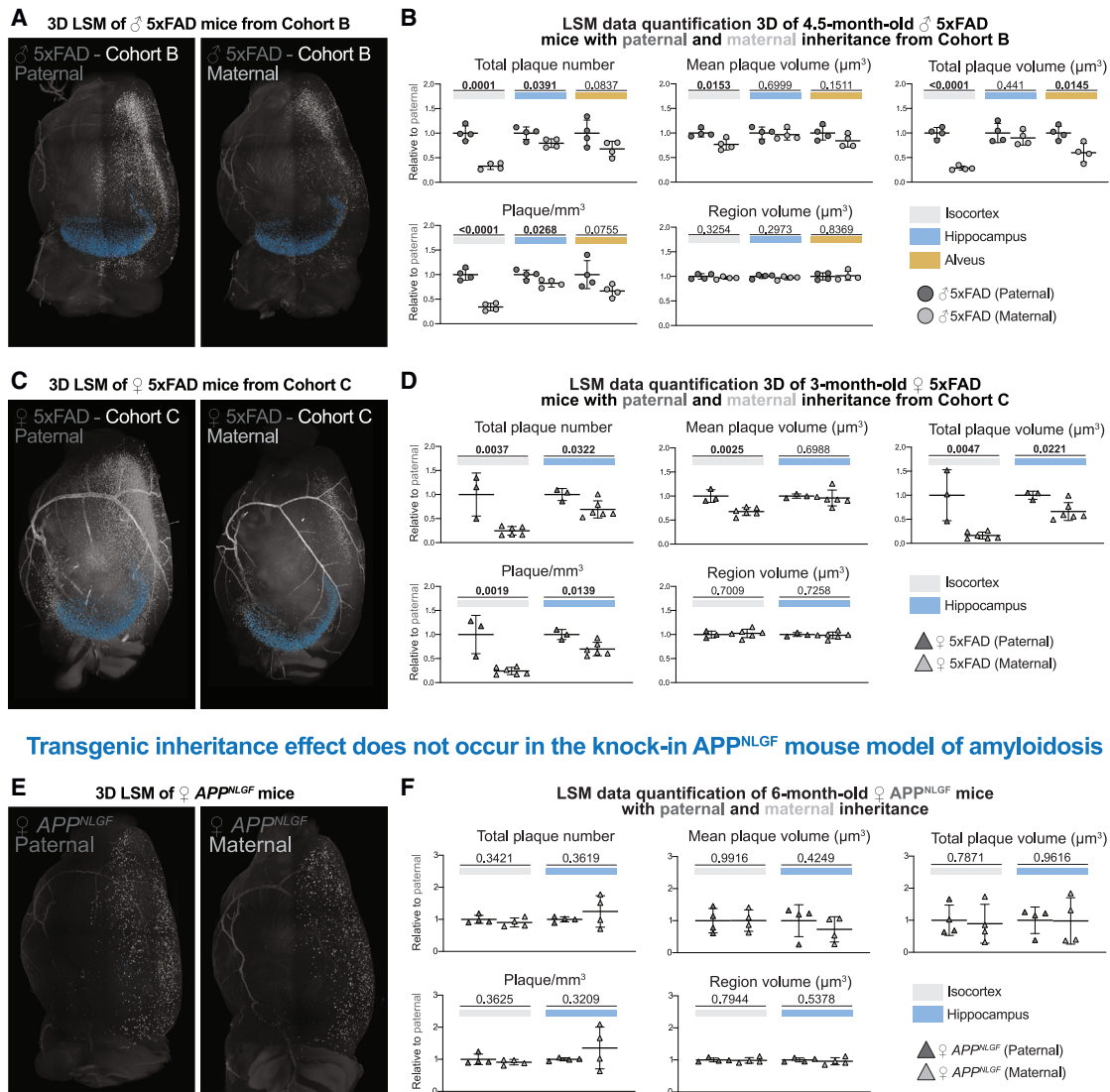
To exclude other associated factors that could mediate our observed effects, we asked whether gestation in or rearing by a 5xFAD dam influences plaque burden in the offspring (Figure S4; [Data S2](#)). For example, an alternative explanation for our findings would be that embryos are exposed to maternal immune priming associated with plaque pathology in the dam,

5xFAD heterozygous breeding matched the plaque burden seen in animals with distinct parental transgenic sources (Figure S4D; [Data S2](#)). From this dataset, we conclude that gestation or rearing by a 5xFAD dam is unlikely the mechanism underlying the lower plaque count seen in 5xFAD animals with a maternal transgenic inheritance.

### Parental transgene source affects *Thy1.2* promoter-driven transgene expression

Genomic imprinting of the transgene would directly influence expression levels of APP. To study this, we hypothesized that the reduced plaque burden in maternal inheritance cohorts is associated with lower amounts of APP. Hence, we performed immunoblotting experiments of 5xFAD hemibrains with different inheritance patterns, probing for APP and its processing enzymes (Figures 3A and 3B). Indeed, we observed that human APP levels are lower in mice with a maternal compared with a paternal inheritance. This held true across immunoblots with

Transgenic inheritance effect is independent of sex, age, and mouse colony of congenic 5xFAD mice



Transgenic inheritance effect does not occur in the knock-in APP<sup>NLGF</sup> mouse model of amyloidosis

**Figure 2. Inheritance pattern influences plaque burden in other 5xFAD colonies but not in APP<sup>NLGF</sup> knockin mice**

(A) LSM 3D visualization of male 5xFAD hemibrains of animals with paternal and maternal inheritance at 4.5 months of age from cohort B. (B) Quantification of male 5xFAD data from cohort B with paternal ( $n = 4$ ) and maternal ( $n = 4$ ) inheritance. Maternal data points were normalized to paternal data. (C) LSM 3D visualization of female 5xFAD hemibrains of animals with paternal and maternal inheritance at 3 months of age from cohort C. (D) Quantification of female 5xFAD data from cohort C with paternal ( $n = 3$ ) and maternal ( $n = 6$ ) inheritance. (E) LSM 3D visualization of female APP<sup>NLGF</sup> hemibrains with paternal and maternal inheritance at 6 months of age. (F) Quantification of female APP<sup>NLGF</sup> data with paternal ( $n = 4$ ) and maternal ( $n = 4$ ) inheritance. (A, C, and E) Color-region allocation is as follows: white, isocortex; blue, hippocampus; and yellow, alveus. (B, D, and F) All data points were normalized to paternal data. Dark gray shapes represent paternal data, and light gray shapes represent maternal data. For each parameter, an unpaired, two-tailed Student's t test was performed ( $p$  values indicated in graphs, significant  $p$  values [ $<0.05$ ] highlighted in bold) comparing paternal with maternal inheritance. Thick lines represent means with SD (thin lines) and individual data points displayed. Raw unnormalized data of quantitative LSM are available in [Data S2](#).

two different human-APP-specific antibodies: 6E10, binding the A $\beta$  region ( $69.76\% \pm 4.33$ ,  $p = 0.0003$ ), and 1D1, binding the N terminus of APP ( $69.96\% \pm 16.36$ ,  $p = 0.0523$ ). Lastly, immunoblotting also revealed unchanged levels of the rate-limiting enzyme in the amyloidogenic pathway,  $\beta$ -secretase 1 (BACE1), further suggesting that the transgenic inheritance pattern modu-

lates APP processing by elevating the abundance of the substrate.

To elucidate whether this effect is also present in other Thy1.2-driven transgenes, we turned to an ATP biosensor line (ATeam)<sup>10</sup> in which the fluorescent-protein-based fluorescence resonance energy transfer (FRET) sensor (CFP-mVenus pair) is also driven

Transgenic inheritance might be due to genomic imprinting of Thy1.2 promoter in germline

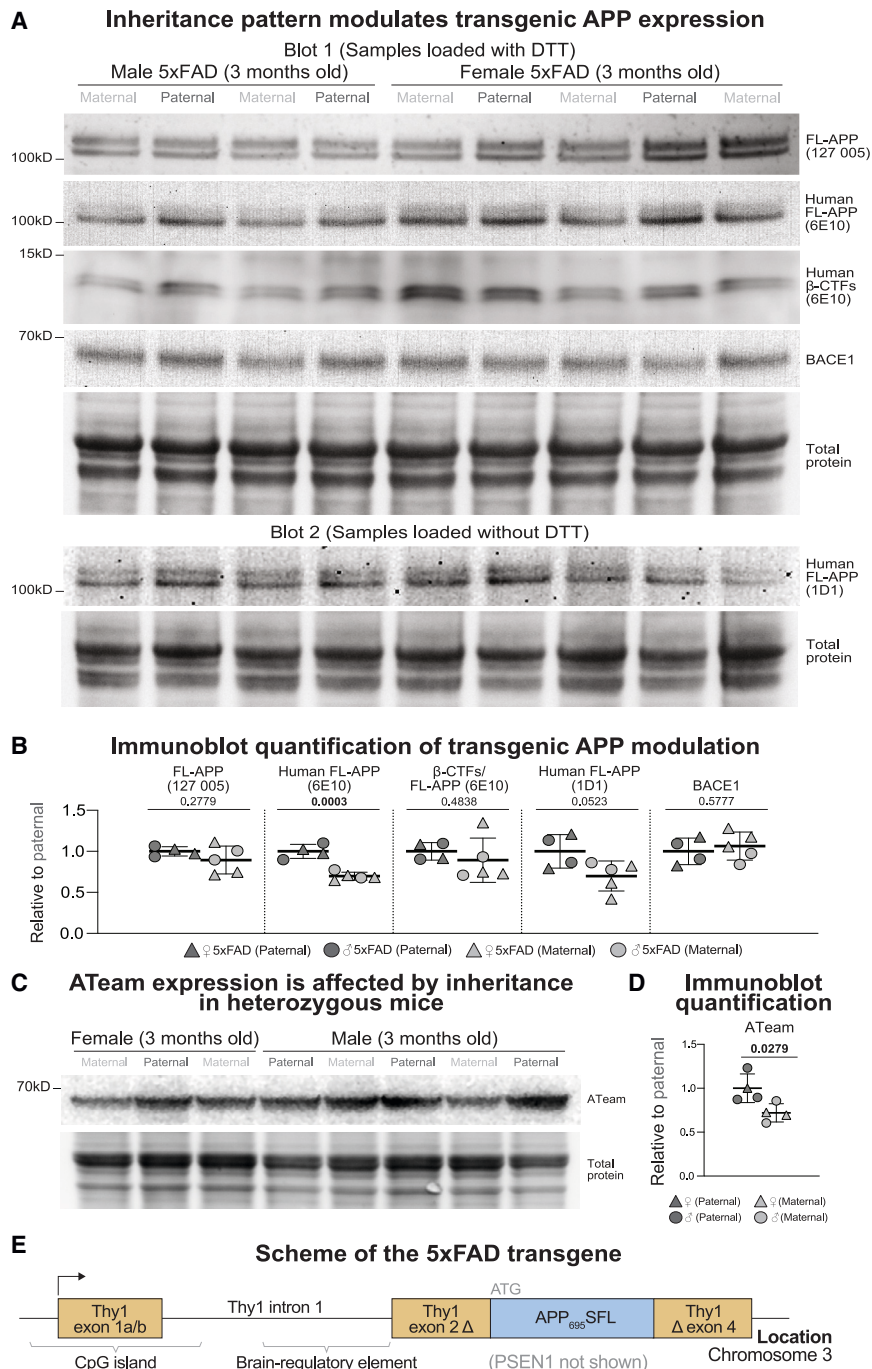


Figure 3. Thy1.2-promoter-driven transgene expression is affected by parental transgenic source

(A) Immunoblots showing amyloidogenic processing components (APP, BACE1) in 3-month-old male ( $n = 4$ ) and female ( $n = 5$ ) 5xFAD mice with different inheritance patterns. (B) Quantification of immunoblots of 5xFAD animals with different parental transgenic sources. (C) Immunoblot showing ATeam protein expression labeled with GFP in 3-month-old male ( $n = 5$ ) and female ( $n = 3$ ) mice with different inheritance patterns. (D) Quantification of immunoblots of ATeam mice with different parental transgenic sources. (A and C) Raw immunoblots are shown in Data S1. (B and D) All data points were normalized to paternal data. Dark gray shapes represent paternal data, and light gray shapes represent maternal data. For each blot, an unpaired, two-tailed Student's  $t$  test was performed ( $p$  values indicated in graphs, significant  $p$  values [ $<0.05$ ] highlighted in bold) comparing paternal with maternal inheritance. Thick lines represent means with SD (thin lines) and individual data points displayed. Source data of immunoblot quantification are available in Data S2. (E) The 5xFAD APP transgene construct, with the Thy1.2 exons and introns, APP insertion site, reported CpG island location, and brain regulatory element highlighted.<sup>9</sup>

genomic imprinting occurs in the Thy1.2 promoter region of transgenic mice, which was previously shown to contain a CpG island<sup>9</sup> (Figure 3E), modulating transgenic protein expression.

Reporting details of experimental 5xFAD animals in literature

In this study, we used the congenic 5xFAD mouse line (Table S1) and reported the modulatory effect of transgenic inheritance on A $\beta$  plaque burden. Notably, our reported effects could also have implications for the original, mixed (C57BL/6 x SJL) hybrids or other backgrounds, given that the 5xFAD model has been used in various crossbreeding schemes in the literature. To better gauge the nature and extent of its use, we reviewed published studies using the 5xFAD mouse line from 2019 to 2024

by a Thy1.2 promoter. We performed immunoblotting experiments for the transgenic sensor expression in mouse brains derived from cohorts with maternal or paternal inheritance of the transgene. Indeed, ATeam mice with a maternal inheritance showed a similarly lower transgene expression ( $71.9\% \pm 15.5$ ,  $p = 0.0279$ ) compared with age- and sex-matched mice with a paternal inheritance (Figures 3C and 3D). These findings in an additional Thy1.2-promoter-driven transgene indicate that

(Table 1; Data S2), as indexed in the PubMed database with “5xFAD” as the search term. We further limited our list to experimental studies that used heterozygous/hemizygous 5xFAD mice, bringing the total to 922 papers.

Although sex dimorphism in the 5xFAD model has been copiously noted,<sup>5–7</sup> 22.8% of studies still pooled male and female mouse data during their analyses. Furthermore, 169 publications (18.3%) did not report the sex of the experimental 5xFAD mice

**Table 1. Systematic review of studies utilizing 5xFAD mice from 2019 to 2024**

Overview of studies utilizing 5xFAD mice in 2019–2024	
Initial PubMed search	991
Excluding reviews, commentaries, and errata	960
Manual exclusion of unsuitable papers	926
Excluding studies using homozygous 5xFAD only	922 (total)
Sex of experimental animals ( <i>n</i> = 922)	
Sex of mice not reported	169 (18.33%)
Males and females pooled	210 (22.78%)
Males only	240 (26.03%)
Females only	145 (15.73%)
Males and females utilized for separate analysis	158 (17.14%)
Strains of experimental animals ( <i>n</i> = 922)	
Congenic C57BL/6 5xFAD	455 (49.35%)
C57BL/6 5xFAD reported	360 (39.05%)
Only control C57BL/6 reported	55 (5.97%)
No number of backcrossing with C57BL/6 reported	40 (4.34%)
Mixed C5BL/6 x SJL 5xFAD	297 (32.21%)
C57BL/6 x SJL 5xFAD reported	288 (31.24%)
Only control C5BL/6 x SJL reported	9 (0.98%)
Both congenic and mixed 5xFAD utilized	1 (0.11%)
Unspecified strain	164 (17.79%)
Other backgrounds	5 (0.54%)
Strains used in crossbreeding studies ( <i>n</i> = 158)	
Congenic C57BL/6	131 (82.91%)
C57BL/6 5xFAD reported	107 (67.72%)
No number of backcrossing with C57BL/6 reported	24 (15.19%)
Mixed C5BL/6 x SJL 5xFAD	6 (3.8%)
Unspecified strain	19 (12.03%)
Other backgrounds	2 (1.27%)
Reporting of source or breeding scheme to generate experimental animals ( <i>n</i> = 922)	
Unspecified sex of 5xFAD breeders	537 (58.24%)
Directly purchased from The Jackson Laboratory	215 (23.32%)
Male 5xFAD x female non-5xFAD (paternal inheritance)	149 (16.16%)
Female 5xFAD x male non-5xFAD (maternal inheritance)	17 (1.84%)
Male 5xFAD x female non-5xFAD/female 5xFAD x male non-5xFAD (pooled inheritance)	4 (0.43%)

Reported parameters include general overview as well as inclusion and exclusion criteria, sex and strains of 5xFAD mice, and transmission of transgene from breeding schemes. The full list of reviewed papers is available in [Data S2](#).

used at all. We conclude that although sex is a known modulator of plaque burden in 5xFAD mice, a large portion of studies still lacked consistency in reporting essential details of experimental animals.

Highlighting the relevance of our current findings on the congenic 5xFAD strain, nearly half of the studies (*n* = 455; 49.4%) opted for the congenic, whereas 32.2% used the original mixed strain. Importantly, the congenic line was used in over 80% of the 158 studies that crossed 5xFAD animals to other models, suggesting that experiments involving 5xFAD crossbreeds may be particularly susceptible to variabilities brought about by our proposed transgenic inheritance effect.

We then evaluated how research groups reported breeding schemes for experimental animals carrying the 5xFAD transgene. Whether using 5xFAD as is or crossing with other mouse models, only 170 of the reviewed studies (18.4%) specified the parental 5xFAD transgenic source of their experimental mice, the majority of which used a paternal breeding setup (16.2% overall; 87.7% of all inheritance-reporting studies), whereas 17 papers described maternal inheritance (1.8% overall; 10.0% of inheritance-reporting studies). Many of the studies that used 5xFAD males as the transgene carrier also noted that this method of breeding has been suggested by the supplier. Accordingly, a paternal inheritance pattern may be likely for studies involving 5xFAD animals that were purchased directly from The Jackson Laboratory without any subsequent breeding in-house (23.3%). Perhaps more strikingly, 4 studies explicitly mentioned using experimental animals derived from a pool of both paternal and maternal 5xFAD transgene transmission. Among these, 3 used the congenic C57BL/6 strain.<sup>11–13</sup> Moreover, as the experimental animals in 3 of these pooled inheritance studies were derived from crossing 5xFAD mice with other models,<sup>11,12,14</sup> studies that crossbreed 5xFAD animals to other lines might be at a higher risk of pooling experimental mice bearing transgenes from different parental sources. By contrast, more than 500 of the reviewed papers—accounting for a staggering 58.2%—did not report the specific sex of the 5xFAD transgene carrier used.

Taken together, our systematic review has revealed variabilities in the reporting of breeding schemes and other parameters when using this model. This suggests that a more consistent reporting may be useful to avoid overlooking confounding factors, such as transgene inheritance, that could affect the interpretation and reproducibility of 5xFAD experimental data or other AD models employing the Thy1 promoter to drive transgene expression ([Data S2](#)).

## DISCUSSION

The 5xFAD mouse model is one of the most used mouse models in AD research and is primarily used to study the impact of experimental interventions on amyloid plaque burden. Several factors, such as age and sex, have been identified to intrinsically modulate plaque burden in 5xFAD cohorts ([Figures S1 and S2](#)). Reducing the within-group variability in 5xFAD mice is essential to correctly interpret plaque burden changes in experimental cohorts. Here, we identify a novel factor that significantly influences plaque burden in 5xFAD mice: the inheritance pattern of the

transgene (Figures 1 and 2). Importantly, the extent of the observed effect is comparable with the known sex dimorphism. Thus, our findings urge the AD research community to (1) systematically report breeding schemes in publications, (2) ensure the comparison of inheritance-matched cohorts, and (3) critically review past publications for inheritance mismatches as a confounding variable.

For example, a study utilizing paternally and maternally inherited 5xFAD animals in the same treatment group or genotype would yield a very variable dataset, leading to false negatives. On the other hand, treatment groups or genetic modifications done on 5xFAD mice with different transgenic sources could lead to false positives. In our systematic review (Table 1), we found that less than 20% of published 5xFAD studies reported the transgenic inheritance of their 5xFAD mice. The transgenic-inheritance-based modulatory effect could conceivably be a large-scale concern, as close to 60% of all 992 reviewed studies did not fully disclose the inheritance pattern of the 5xFAD transgene in their mice. This substantial proportion of non-inheritance-reporting studies may highlight the lack of publicly available information and scientific consensus regarding the importance of maintaining a consistent breeding scheme for this model. Additionally, we observed that the congenic C57BL/6 5xFAD line is the background most often used (around 50% of all studies), especially for crossbreeding experiments, due to the abundance of other genetically modified models being raised on the C57BL/6 background. Although our present findings were made using congenic 5xFAD mice, similar experiments are, however, necessary to further validate this inheritance effect in the mixed C57BL/6 x SJL strain, given that it is the original strain of the model and the reported differences in amyloid deposition between 5xFAD mice with the congenic and mixed backgrounds.<sup>15</sup>

Based on our findings, we recommend breeding and maintaining 5xFAD mice by inheriting the transgene through only one germ line—for example, paternally—when a more rapid plaque deposition is desired. In studies where a more protracted plaque accumulation rate is desirable, consecutive maternal inheritance can be utilized; for instance, probing for phenomena that are age-dependent. Additionally, the delayed plaque deposition would provide a wider time window for testing interventions such as drugs—the administration of which is often time-critical for eliciting their desired effects.

What could be driving our proposed transgenic inheritance effect? Our negative findings in heterozygote 5xFAD breeding pairs (Figure S4) and *APP<sup>NLGF</sup>* mice (Figures 2E and 2F), as well as the identified APP expression level differences (Figure 3), all point toward genomic imprinting as the potential mechanism for the inheritance effect. In this scenario, the transgene could be epigenetically modified in the female germ line, leading to reduced expression. For instance, undermethylation is classically associated with increased gene expression.<sup>16</sup> Indeed, studies have reported epigenetic-mediated changes of transgenes resulting in distinct transgenic activity<sup>17</sup> and described methylation pattern differences depending on parental origin.<sup>18–22</sup> The 5xFAD transgene could undergo imprinting either because it integrated in a genomic

region that is normally imprinted<sup>23</sup> or the transgene components could be imprinted irrespective of their genetic location. Our observation of a similar attenuation of expression levels in ATeam mice with a maternal inheritance argues for the latter and nominates the shared Thy1.2 promoter region as a potentially imprinted region.

As described, the 5xFAD transgene consists of mutated APP and PSEN1 versions, both driven by a Thy1.2 promoter, a widely used promoter to induce transgene expression in neurons.<sup>24</sup> In 5xFAD mice, the two transgenes were inserted in a single locus on chromosome 3, specifically chr3:6297836.<sup>25</sup> Interestingly, the Thy1 locus was shown to contain CpG sites around the transcriptional start site extending to intron 1,<sup>26</sup> which is part of the Thy1.2 promoter construct.<sup>27–30</sup> We are not aware of a study that explicitly investigated allele-specific expression level differences of endogenous Thy1 in the brain. However, it has been shown that methylation changes in the CpG island region of Thy1 contribute to the regulation of Thy1 expression in the context of lung fibrosis,<sup>26</sup> cancer,<sup>31,32</sup> and adipogenesis.<sup>33</sup> It is also known to a certain extent, however, that the genomic environment impacts transgene expression levels in Thy1.2-driven transgenes. For example, transgenic mice that carry Thy1.2-promoter-driven fluorescent protein have been shown to exhibit remarkably different expression patterns.<sup>34</sup>

Our findings underscore the need to stringently monitor breeding schemes of other widely used AD mouse models using the Thy1.2 promoter, such as the Tg-SwDI<sup>35</sup> or the APPPS1<sup>36</sup> models of amyloidosis, as well as the P301L<sup>37</sup> model of tauopathy (Data S2). Epigenetic screening of the Thy1.2 promoter region in neurons could provide a definitive answer regarding whether methylation patterns differ based on the parental source of the transgene.

Ultimately, our experimental data and systematic review affirm the urgent need for studies utilizing the 5xFAD model to maintain a consistent breeding scheme. We believe that breeding schemes should be reported on the same level as the sex of animals to encourage transparency and reproducibility. We hope that our data could further mitigate discrepancies in preclinical AD research arising from variabilities that could be explained and managed, such as our proposed transgenic inheritance effect.

## RESOURCE AVAILABILITY

### Lead contact

Further information and requests for reagents may be directed to and will be fulfilled by the lead contact, Dr. Constanze Depp ([depp@broadinstitute.org](mailto:depp@broadinstitute.org)).

### Materials availability

This study did not generate new, unique reagents or mouse lines.

### Data and code availability

- All data reported in this paper will be shared by the lead contact upon request.
- This paper does not report original code.
- Any additional information required to reanalyze the data reported in this paper is available from the lead contact upon request.

## ACKNOWLEDGMENTS

The authors express their gratitude to the staff at the animal facility of the Max Planck Institute for Multidisciplinary Sciences (MPI-NAT), City Campus. The authors also acknowledge Annette Fahrenholz and Carolin Boehler for their technical assistance in sample preparation for biochemical and imaging experiments, alongside members of the KAGS subgroup and the Department of Neurogenetics for their scientific input. The authors also extend their appreciation to Oliver Wirths and Bastian Bues for valuable scientific discussions. H.J.B. was supported by a training grant in the Molecular Biology of Neurodegeneration and Alzheimer's Disease (5T32AG000222). The authors thank the neurobiology imaging facility at Harvard Medical School, Boston (Harvard Medical School Neurobiology Imaging Core Facility, RRID:SCR\_009808) for providing access to a light-sheet microscope. The research described in this manuscript was primarily conducted in K.-A.N.'s laboratory and was supported by the Deutsche Forschungsgemeinschaft (DFG, TRR274), the Dr. Myriam and Sheldon Adelson Medical Foundation (AMRF), and an ERC Advanced Grant (MyelinANO).

## AUTHOR CONTRIBUTIONS

A.O.S., C.D., and K.-A.N. conceptualized and designed the experiments. A.O.S. and C.D. planned and executed pilot experiments to verify initial transgenic inheritance effects. A.O.S., E.C.O., and T.N. harvested tissue and performed imaging experiments. A.O.S. and E.C.O. conducted a systematic review of 5xFAD studies. A.O.S., E.C.O., S.M., L.K., and V.H. carried out western blotting. M.T. performed statistical modeling and prepared the pipeline to segment imaging data. L.S., S.A.B., and M.S. provided 5xFAD brains from cohort B. C.D., H.J.B., M.H., and B.S. provided 5xFAD brains and imaging data from cohort C. V.H. assisted in sample collection and data analysis. F.B. carried out genotyping. J.H. provided the ATeam mice and valuable scientific input. A.O.S. performed data analysis and constructed all figures. A.O.S., E.C.O., and M.T. carried out copyediting and proofreading of the manuscript. A.O.S., C.D., and K.-A.N. prepared the manuscript.

## DECLARATION OF INTERESTS

The authors declare no competing interests.

## STAR★METHODS

Detailed methods are provided in the online version of this paper and include the following:

- KEY RESOURCES TABLE
- EXPERIMENTAL MODELS
  - Animal husbandry
- METHOD DETAILS
  - Tissue preparation
  - Tissue clearing and labeling
  - Light-sheet imaging and analysis
  - Protein extraction
  - Immunoblotting
  - Data analysis, statistics, and figure preparation
  - Systematic review of 5xFAD studies
  - Reporting of Thy1 promoter-driven transgenic AD models

## SUPPLEMENTAL INFORMATION

Supplemental information can be found online at <https://doi.org/10.1016/j.neuron.2024.12.025>.

Received: July 9, 2024

Revised: November 18, 2024

Accepted: December 23, 2024

Published: January 20, 2025

## REFERENCES

1. Oakley, H., Cole, S.L., Logan, S., Maus, E., Shao, P., Craft, J., Guillozet-Bongaarts, A., Ohno, M., Disterhoft, J., Van Eldik, L., et al. (2006). Intraneuronal beta-amyloid aggregates, neurodegeneration, and neuron loss in transgenic mice with five familial Alzheimer's disease mutations: potential factors in amyloid plaque formation. *J. Neurosci.* 26, 10129–10140. <https://doi.org/10.1523/JNEUROSCI.1202-06.2006>.
2. Ohno, M., Chang, L., Tseng, W., Oakley, H., Citron, M., Klein, W.L., Vassar, R., and Disterhoft, J.F. (2006). Temporal memory deficits in Alzheimer's mouse models: rescue by genetic deletion of BACE1. *Eur. J. Neurosci.* 23, 251–260. <https://doi.org/10.1111/j.1460-9568.2005.04551.x>.
3. Depp, C., Sun, T., Sasmita, A.O., Spieth, L., Berghoff, S.A., Nazarenko, T., Overhoff, K., Steixner-Kumar, A.A., Subramanian, S., Arinrad, S., et al. (2023). Myelin dysfunction drives amyloid-beta deposition in models of Alzheimer's disease. *Nature* 618, 349–357. <https://doi.org/10.1038/s41586-023-06120-6>.
4. Burgold, S., Filser, S., Dorostkar, M.M., Schmidt, B., and Herms, J. (2014). In vivo imaging reveals sigmoidal growth kinetic of beta-amyloid plaques. *Acta Neuropathol. Commun.* 2, 30. <https://doi.org/10.1186/2051-5960-2-30>.
5. Fisher, D.W., Bennett, D.A., and Dong, H. (2018). Sexual dimorphism in predisposition to Alzheimer's disease. *Neurobiol. Aging* 70, 308–324. <https://doi.org/10.1016/j.neurobiolaging.2018.04.004>.
6. Forner, S., Kawachi, S., Balderrama-Gutierrez, G., Kramár, E.A., Matheos, D.P., Phan, J., Javonillo, D.I., Tran, K.M., Hingco, E., da Cunha, C., et al. (2021). Systematic phenotyping and characterization of the 5xFAD mouse model of Alzheimer's disease. *Sci. Data* 8, 270. <https://doi.org/10.1038/s41597-021-01054-y>.
7. Sil, A., Erfani, A., Lamb, N., Copland, R., Riedel, G., and Platt, B. (2022). Sex Differences in Behavior and Molecular Pathology in the 5xFAD Model. *J. Alzheimers Dis.* 85, 755–778. <https://doi.org/10.3233/JAD-210523>.
8. Bordeleau, M., Lacabanne, C., Fernández de Cossío, L., Vernoux, N., Savage, J.C., González-Ibáñez, F., and Tremblay, M.É. (2020). Microglial and peripheral immune priming is partially sexually dimorphic in adolescent mouse offspring exposed to maternal high-fat diet. *J. Neuroinflammation* 17, 264. <https://doi.org/10.1186/s12974-020-01914-1>.
9. Spanopoulou, E., Giguere, V., and Grosveld, F. (1988). Transcriptional unit of the murine Thy-1 gene: different distribution of transcription initiation sites in brain. *Mol. Cell. Biol.* 8, 3847–3856. <https://doi.org/10.1128/mcb.8.9.3847-3856.1988>.
10. Trevisiol, A., Saab, A.S., Winkler, U., Marx, G., Imamura, H., Möbius, W., Kusch, K., Nave, K.-A., and Hirtlinger, J. (2017). Monitoring ATP dynamics in electrically active white matter tracts. *eLife* 6, e24241. <https://doi.org/10.7554/eLife.24241>.
11. Valencia-Olvera, A.C., Balu, D., Bellur, S., McNally, T., Saleh, Y., Pham, D., Ghura, S., York, J., Johansson, J.O., LaDu, M.J., et al. (2023). A novel apoE-mimetic increases brain apoE levels, reduces A $\beta$  pathology and improves memory when treated before onset of pathology in male mice that express APOE3. *Alzheimers Res. Ther.* 15, 216. <https://doi.org/10.1186/s13195-023-01353-z>.
12. Lucero, E.M., Freund, R.K., Smith, A., Johnson, N.R., Dooling, B., Sullivan, E., Prikhodko, O., Ahmed, M.M., Bennett, D.A., Hohman, T.J., et al. (2022). Increased KIF11/kinesin-5 expression offsets Alzheimer A $\beta$ -mediated toxicity and cognitive dysfunction. *iScience* 25, 105288. <https://doi.org/10.1016/j.isci.2022.105288>.
13. Bosch, M.E., Dodiya, H.B., Michalkiewicz, J., Lee, C., Shaik, S.M., Weigle, I.Q., Zhang, C., Osborn, J., Nambiar, A., Patel, P., et al. (2024). Sodium oligomannate alters gut microbiota, reduces cerebral amyloidosis and reactive microglia in a sex-specific manner. *Mol. Neurodegener.* 19, 18. <https://doi.org/10.1186/s13024-023-00700-w>.
14. Oh, Y., Lee, W., Kim, S.H., Lee, S., Kim, B.C., Lee, K.H., Kim, S.H., and Song, W.K. (2022). SPIN90 Deficiency Ameliorates Amyloid  $\beta$

- Accumulation by Regulating APP Trafficking in AD Model Mice. *Int. J. Mol. Sci.* 23, 10563. <https://doi.org/10.3390/ijms231810563>.
15. Neuner, S.M., Heuer, S.E., Huentelman, M.J., O'Connell, K.M.S., and Kaczorowski, C.C. (2019). Harnessing Genetic Complexity to Enhance Translatability of Alzheimer's Disease Mouse Models: A Path toward Precision Medicine. *Neuron* 107, 399–411.e5. <https://doi.org/10.1016/j.neuron.2018.11.040>.
  16. Naveh-Many, T., and Cedar, H. (1981). Active gene sequences are under-methylated. *Proc. Natl. Acad. Sci. USA* 78, 4246–4250. <https://doi.org/10.1073/pnas.78.7.4246>.
  17. Chaillet, J.R., Vogt, T.F., Beier, D.R., and Leder, P. (1991). Parental-specific methylation of an imprinted transgene is established during gametogenesis and progressively changes during embryogenesis. *Cell* 66, 77–83. [https://doi.org/10.1016/0092-8674\(91\)90140-t](https://doi.org/10.1016/0092-8674(91)90140-t).
  18. Reik, W., Collicch, A., Norris, M.L., Barton, S.C., and Surani, M.A. (1987). Genomic imprinting determines methylation of parental alleles in transgenic mice. *Nature* 328, 248–251. <https://doi.org/10.1038/328248a0>.
  19. Sapienza, C., Peterson, A.C., Rossant, J., and Balling, R. (1987). Degree of methylation of transgenes is dependent on gamete of origin. *Nature* 328, 251–254. <https://doi.org/10.1038/328251a0>.
  20. Sasaki, H., Hamada, T., Ueda, T., Seki, R., Higashinakagawa, T., and Sakaki, Y. (1991). Inherited type of allelic methylation variations in a mouse chromosome region where an integrated transgene shows methylation imprinting. *Development* 111, 573–581. <https://doi.org/10.1242/dev.111.2.573>.
  21. Swain, J.L., Stewart, T.A., and Leder, P. (1987). Parental legacy determines methylation and expression of an autosomal transgene: a molecular mechanism for parental imprinting. *Cell* 50, 719–727. [https://doi.org/10.1016/0092-8674\(87\)90330-8](https://doi.org/10.1016/0092-8674(87)90330-8).
  22. Ueda, T., Yamazaki, K., Suzuki, R., Fujimoto, H., Sasaki, H., Sakaki, Y., and Higashinakagawa, T. (1992). Parental methylation patterns of a transgenic locus in adult somatic tissues are imprinted during gametogenesis. *Development* 116, 831–839. <https://doi.org/10.1242/dev.116.4.831>.
  23. DeLoia, J.A., and Solter, D. (1990). A transgene insertional mutation at an imprinted locus in the mouse genome. *Development* 108, 73–79. <https://doi.org/10.1242/dev.108.Supplement.73>.
  24. Campsall, K.D., Mazerolle, C.J., De Repentingy, Y., Kothary, R., and Wallace, V.A. (2002). Characterization of transgene expression and Cre recombinase activity in a panel of Thy-1 promoter-Cre transgenic mice. *Dev. Dyn.* 224, 135–143. <https://doi.org/10.1002/dvdy.10092>.
  25. Goodwin, L.O., Splinter, E., Davis, T.L., Urban, R., He, H., Braun, R.E., Chesler, E.J., Kumar, V., van Min, M., Ndukum, J., et al. (2019). Large-scale discovery of mouse transgenic integration sites reveals frequent structural variation and insertional mutagenesis. *Genome Res.* 29, 494–505. <https://doi.org/10.1101/gr.233866.117>.
  26. Sanders, Y.Y., Pardo, A., Selman, M., Nuovo, G.J., Tollefsbol, T.O., Siegal, G.P., and Hagood, J.S. (2008). Thy-1 Promoter Hypermethylation: A Novel Epigenetic Pathogenic Mechanism in Pulmonary Fibrosis. *Am. J. Respir. Cell Mol. Biol.* 39, 610–618. <https://doi.org/10.1165/rcmb.2007-0322OC>.
  27. Sneller, M.C., and Gunter, K.C. (1987). DNA methylation alters chromatin structure and regulates Thy-1 expression in EL-4 T cells. *J. Immunol.* 138, 3505–3512. <https://doi.org/10.4049/jimmunol.138.10.3505>.
  28. Gundersen, G., Kolstø, A.B., Larsen, F., and Prydz, H. (1992). Tissue-specific methylation of a CpG island in transgenic mice. *Gene* 113, 207–214. [https://doi.org/10.1016/0378-1119\(92\)90397-8](https://doi.org/10.1016/0378-1119(92)90397-8).
  29. Szyf, M., Tanigawa, G., and McCarthy, P.L. (1990). A DNA Signal from the Thy-1 Gene Defines De Novo Methylation Patterns in Embryonic Stem Cells. *Mol. Cell. Biol.* 10, 4396–4400. <https://doi.org/10.1128/mcb.10.8.4396-4400.1990>.
  30. Richard Albert, J., Au Yeung, W.K., Toriyama, K., Kobayashi, H., Hirasawa, R., Brind'Amour, J., Bogutz, A., Sasaki, H., and Lorincz, M. (2020). Maternal DNMT3A-dependent de novo methylation of the paternal genome inhibits gene expression in the early embryo. *Nat. Commun.* 11, 5417. <https://doi.org/10.1038/s41467-020-19279-7>.
  31. Lung, H.L., Bangarusamy, D.K., Xie, D., Cheung, A.K.L., Cheng, Y., Kumaran, M.K., Miller, L., Liu, E.T.-B., Guan, X.-Y., Sham, J.S., et al. (2005). THY1 is a candidate tumour suppressor gene with decreased expression in metastatic nasopharyngeal carcinoma. *Oncogene* 24, 6525–6532. <https://doi.org/10.1038/sj.onc.1208812>.
  32. Montanari, M., Carbone, M.R., Coppola, L., Giuliano, M., Arpino, G., Lauria, R., Nardone, A., Leccia, F., Trivedi, M.V., Garbi, C., et al. (2019). Epigenetic Silencing of THY1 Tracks the Acquisition of the Notch1-EGFR Signaling in a Xenograft Model of CD44<sup>+</sup>/CD24<sup>low</sup>/CD90<sup>+</sup> Myoepithelial Cells. *Mol. Cancer Res.* 17, 628–641. <https://doi.org/10.1158/1541-7786.MCR-17-0324>.
  33. Flores, E.M., Woeller, C.F., Falsetta, M.L., Susiarjo, M., and Phipps, R.P. (2019). Thy1 (CD90) expression is regulated by DNA methylation during adipogenesis. *FASEB J.* 33, 3353–3363. <https://doi.org/10.1096/fj.201801481R>.
  34. Feng, G., Mellor, R.H., Bernstein, M., Keller-Peck, C., Nguyen, Q.T., Wallace, M., Nerbonne, J.M., Lichtman, J.W., and Sanes, J.R. (2000). Imaging neuronal subsets in transgenic mice expressing multiple spectral variants of GFP. *Neuron* 28, 41–51. [https://doi.org/10.1016/s0896-6273\(00\)00084-2](https://doi.org/10.1016/s0896-6273(00)00084-2).
  35. Davis, J., Xu, F., Deane, R., Romanov, G., Previti, M.L., Zeigler, K., Zlokovic, B.V., and Van Nostrand, W.E. (2004). Early-onset and Robust Cerebral Microvascular Accumulation of Amyloid  $\beta$ -Protein in Transgenic Mice Expressing Low Levels of a Vasculotropic Dutch/Iowa Mutant Form of Amyloid  $\beta$ -Protein Precursor. *J. Biol. Chem.* 279, 20296–20306. <https://doi.org/10.1074/jbc.M312946200>.
  36. Radde, R., Bolmont, T., Kaeser, S.A., Coomaraswamy, J., Lindau, D., Stoltze, L., Calhoun, M.E., Jäggi, F., Wolburg, H., Gengler, S., et al. (2006). Abeta42-driven cerebral amyloidosis in transgenic mice reveals early and robust pathology. *EMBO Rep.* 7, 940–946. <https://doi.org/10.1038/sj.embor.7400784>.
  37. Götz, J., Chen, F., Van Dorpe, J., and Nitsch, R.M. (2001). Formation of Neurofibrillary Tangles in P301L Tau Transgenic Mice Induced by A $\beta$ 42 Fibrils. *Science* 293, 1491–1495. <https://doi.org/10.1126/science.1062097>.
  38. Zhao, J., Fu, Y., Yasvoina, M., Shao, P., Hitt, B., O'Connor, T., Logan, S., Maus, E., Citron, M., Berry, R., et al. (2007). Beta-site amyloid precursor protein cleaving enzyme 1 levels become elevated in neurons around amyloid plaques: implications for Alzheimer's disease pathogenesis. *J. Neurosci.* 27, 3639–3649. <https://doi.org/10.1523/JNEUROSCI.4396-06.2007>.
  39. Singmann, H., Bolker, B., Westfall, J., Aust, F., and Ben-Schachar, M.S. (2024). afex: Analysis of Factorial Experiments. <https://cran.r-project.org/web/packages/afex/afex.pdf>.
  40. Schindelin, J., Arganda-Carreras, I., Frise, E., Kaynig, V., Longair, M., Pietzsch, T., Preibisch, S., Rueden, C., Saalfeld, S., Schmid, B., et al. (2012). Fiji: an open-source platform for biological-image analysis. *Nat. Methods* 9, 676–682. <https://doi.org/10.1038/nmeth.2019>.
  41. Saito, T., Matsuba, Y., Mihira, N., Takano, J., Nilsson, P., Itohara, S., Iwata, N., and Saido, T.C. (2014). Single App knock-in mouse models of Alzheimer's disease. *Nat. Neurosci.* 17, 661–663. <https://doi.org/10.1038/nn.3697>.

## STAR★METHODS

### KEY RESOURCES TABLE

REAGENT or RESOURCE	SOURCE	IDENTIFIER
<b>Antibodies</b>		
APP	Synaptic Systems	Cat#127-005; RRID:AB_2832229
APP (1D1)	Merck	Cat#MABN2287; RRID:AB_3665093
A $\beta$ (6E10)	BioLegend	Cat#803001;RRID:AB_2564653
BACE1 (3D5)	Dr. Robert Vassar <sup>38</sup>	N/A
GFP	Aves Labs	Cat#GFP-1010;RRID:AB_2307313
Alexa 488 g $\alpha$ -mouse	Thermo Fisher	Cat#A-11001; RRID:AB_2534069
HRP g $\alpha$ -mouse	Dianova	Cat#115-035-146; RRID:AB_2307392
HRP g $\alpha$ -rabbit	Dianova	Cat#111-035-045; RRID:AB_2337938
HRP g $\alpha$ -rat	Dianova	Cat#112-035-167, RRID:AB_2338139
<b>Experimental models: Organisms/strains</b>		
Mouse: B6.Cg-Tg(APPswF1L <sub>on</sub> , PSEN1* <sup>M146L</sup> *L286V)6799Vas/Mmjax	The Jackson Laboratory	Strain#034848
Mouse: B6N.Cg-Tg(APPswF1L <sub>on</sub> , PSEN1* <sup>M146L</sup> *L286V)6799Vas/Mmjax	In this study. Obtained by backcrossing B6SJL 5xFAD (The Jackson Laboratory) with C57BL/6N mice.	Original: Strain#034840
Mouse: B6J.Cg-Tg(APPswF1L <sub>on</sub> , PSEN1* <sup>M146L</sup> *L286V)6799Vas/Mmjax	In this study. Obtained by backcrossing B6SJL 5xFAD (The Jackson Laboratory) with C57BL/6J mice.	Original: Strain#034840
Mouse: B6-Tg(Thy1.2-ATeam1.03 <sup>YEMK</sup> )AJhi	Trevisiol et al. <sup>10</sup>	N/A
<b>Software and algorithms</b>		
Adobe Illustrator v29.0.1	Adobe	<a href="https://www.adobe.com/de/products/illustrator.html">https://www.adobe.com/de/products/illustrator.html</a>
Arivis Vision4D v3.2, v4.0	Zeiss	<a href="https://www.zeiss.de">https://www.zeiss.de</a>
Afex package	Singmann et al. <sup>39</sup>	<a href="https://cran.r-project.org/web/packages/afex/index.html">https://cran.r-project.org/web/packages/afex/index.html</a>
FIJI	Schindelin et al. <sup>40</sup>	<a href="https://imagej.net/Fiji">https://imagej.net/Fiji</a>
GraphPad Prism 10	GraphPad Software, Inc.	<a href="https://www.graphpad.com/">https://www.graphpad.com/</a>
InspectorPro v.7.124	LaVision	<a href="https://www.lavision.de/en/">https://www.lavision.de/en/</a>
R v4.3.2	R Core Team	<a href="https://posit.co/download/rstudio-desktop/">https://posit.co/download/rstudio-desktop/</a>
<b>Others</b>		
Congo red	Sigma	Cat#C6767
Fastgreen FCF	Serva	Cat#21295
Western Lightning Plus ECL Oxidizing Reagent Plus and Enhanced Luminol Reagent Plus	PerkinElmer	Cat#NEL103001EA
SuperSignal™ West Femto Maximum Sensitivity Substrate	Thermo Fisher	Cat#34095
Novex™ Tris-Glycine Mini Protein Gels, 4–12%, 1.0 mm, WedgeWell™ format	Novex	Cat#XP04122BOX
Novex™ Tricine Mini Protein Gels, 10 to 20%, 1.0 mm	Novex	Cat#EC66252BOX

### EXPERIMENTAL MODELS

#### Animal husbandry

Animal experiments were carried out in accordance with German and American regulations on animal welfare and were approved by the relevant local authorities (Licenses: 33.19-42502-04-19/3116, 24\_KAN\_0024\_FFDE, and 23\_JHI\_0001\_THYATP.) All

experimental mice were classified as unburdened. Heterozygous 5xFAD,<sup>1</sup> heterozygous *APP<sup>NLGF</sup>*,<sup>41</sup> and ATeam<sup>10</sup> mice of both sexes were utilized in this study as stated in further details in corresponding figure legends. Further details regarding 5xFAD mice utilized for the experiments can be found in Table S1. All 5xFAD mice utilized in this study are on the congenic C57BL/6 background. Experimental 5xFAD animals are generated by: 1) Existing maintenance breeding with C57BL/6 mice negative for the 5xFAD transgene at the animal facility of the Max Planck Institute for Multidisciplinary Sciences, City Campus, in Göttingen (main cohort) or at the German Center for Neurodegenerative Diseases (DZNE, cohort B) in Munich, or 2) By breeding of congenic 5xFAD mice purchased from The Jackson Laboratory (MMRC stock 034848) with C57BL/6 mice.

Experimental animals with a paternal inheritance were generated by breeding male 5xFAD mice with WT females, while mice with a maternal inheritance were generated by breeding female 5xFAD mice with WT males. To probe for differences in 5xFAD plaque load due to age and sex, only mice with a paternal inheritance were analyzed. The same breeding scheme applied for the generation of *APP<sup>NLGF</sup>* mice with different knock-in inheritance patterns. Male and female 5xFAD mice were bred to generate offspring of heterozygous breeding pairs for one arm of the study. ATeam mice are housed at the animal facility of the Max Planck Institute for Multidisciplinary Sciences, City Campus, in Göttingen. Generation of ATeam mice with distinct transgenic inheritance patterns were carried out by breeding either male or female homozygous ATeam mice with WT animals. Genotyping was conducted using ear clips following standard procedures (refer to the original mouse strains for detailed protocols). Genotypes were confirmed by re-genotyping from tail biopsies after euthanasia at the conclusion of each experiment. Mice were housed in groups at the animal facility, following a 12-hour dark-light cycle and provided food without restriction. Ages of animals are specified in the corresponding figure caption and legend.

## METHOD DETAILS

### Tissue preparation

Animals were euthanized by Avertin anesthesia or CO<sub>2</sub> overdose and transcardially flushed with cold phosphate-buffered saline (PBS) or HBSS until the liver was completely decolorized. Upon brain extraction for the main cohort, one hemisphere was then immersed in 4% paraformaldehyde (PFA) in 0.1 M phosphate buffer for fixation and stored long-term in PBS. The remaining hemisphere was then snap-frozen and stored at -80°C until further biochemical experiments. Both hemispheres were collected for imaging experiments for cohort B and C.

### Tissue clearing and labeling

Fixed tissues underwent preparation for LSM imaging using a modified iDISCO protocol, as detailed in our previous work.<sup>3</sup> Hemibrains were initially placed in 2 ml tubes and underwent a series of methanol washes in PBS (50%, 80%, 100% twice, 1 hour each) to gradually dehydrate them. To minimize autofluorescence, hemibrains were then immersed overnight at 4°C in a mixture of dimethyl sulfoxide (DMSO), 30% H<sub>2</sub>O<sub>2</sub>, and methanol. Subsequently, the samples were dehydrated further in 100% methanol for varying durations at different temperatures before being stored overnight at 4°C. The following day, the solution was replaced with 20% DMSO in methanol for 2 hours, followed by a reverse methanol wash in PBS (80%, 50%, 0%, 1 hour each) and a pre-permeabilization step with 0.2% Triton X-100 in PBS for 2 hours. Samples were then permeabilized overnight at 37°C in a solution containing 20% DMSO, 0.2% Triton X-100, and glycine dissolved in PBS. Afterwards, the samples underwent several washes in a PBS solution containing Tween-20, heparin, and sodium azide (2 hours each) before a 72-hour incubation at 37°C in a solution of Congo red dye. Following labeling, hemibrains were rinsed in PTwH and underwent a final methanol wash in PBS (20%, 40%, 60%, 80%, 100%, 1 hour each) followed by overnight incubation in a mixture of methanol and dichloromethane (DCM). Finally, the samples were immersed in DCM for a 1 h 40 min before being cleared in ethyl cinnamate (ECI) for imaging. LSM imaging took place in a sample chamber containing ECI. It is worth noting that some cleared samples, after LSM imaging, were treated with methanol and subjected to paraffin embedding before tissue sectioning to generate 2D slices. All incubation steps were conducted at room temperature unless otherwise specified.

### Light-sheet imaging and analysis

Cleared hemibrains underwent imaging using an LSM setup (UltraMicroscope II, LaVision Biotec) equipped with a corrected dipping cap and a 2x objective lens magnification. InspectorPro software (v.7.124, LaVision Biotec) was used to image samples in mosaic acquisition mode, with: 5 μm light sheet thickness, 30% sheet width, 0.154 sheet numerical aperture, 4 μm z-step size, 2,150 × 2,150 pixels field of view, dynamic focus steps of 5, dual light sheet illumination, and a camera exposure time of 100 ms. Fluorescence was captured using 561 nm laser excitation at 80% laser power and a 585/40 nm emission filter.

Image stacks were stitched using Vision4D software (v3.2, Arivis). Regions of interest (ROIs) in this study comprised the isocortex, hippocampus, and alveus, delineated based on anatomical landmarks. To perform plaque segmentation on 5xFAD hemibrains, a blob finder algorithm in Vision4D was utilized with the following parameters: 15 μm object size, 5-10% probability threshold, and 0% split sensitivity. Imaging and staining artifacts, including arterial staining or intracellular lipofuscin accumulations in cells are excluded by size and structure. For plaque analysis of *APP<sup>NLGF</sup>* hemibrains, a machine learning approach was employed for 3D shape recognition based on 2D inputs, utilizing 200 desired objects (plaques) and backgrounds (non-plaque structures). Training inputs were generated using the brush tool at size 5 and 100% magnification. Subsequently, segment

colocalization was conducted to identify plaques within specific ROIs. Noise reduction involved deleting objects with voxel sizes ranging from 1 to 10 and plane counts from 1 to 3, as these mostly represented non-specifically stained structures or residual blood artifacts from perfusion. Finally, object metadata and correlated features were exported as spreadsheets for further statistical analysis and data representation.

Light sheet imaging of cohort C was performed at the Neurobiology Imaging Facility with slightly modified imaging parameters to imaging performed in the main cohort (magnification 1x, 100% sheet width, 4  $\mu\text{m}$  light sheet thickness, 4  $\mu\text{m}$  Z-step size, full field of view, 15 dynamic focus steps, no tiling, one-sided light sheet illumination, 70% laser intensity 561nm laser line, 100ms exposure time). The analysis was performed using Vision4D (v4.0, Arivis) and plaques were segmented using the machine learning segmenter that was trained on multiple datasets. Segments under 100  $\mu\text{m}$  in size were considered noise and removed from the dataset. Plaques in 5x*FAD* hemibrains were rendered in 3D as centroids with a uniform size while *APP<sup>NLGF</sup>* plaques were rendered as their respective surface models.

### Protein extraction

Frozen hemibrains were placed in RIPA buffer containing 20 mM Tris-HCl pH 7.5, 150 mM NaCl, 1% NP-40, 1% SDS, 2.5 mM sodium pyrophosphate and 1 mM  $\text{Na}_2\text{EDTA}$  and homogenized with the Precellys bead-milling method (Precellys). Homogenization was conducted at 4°C with the following parameters: centrifugation at 6500 g twice for 30 s each, with a 15 s pause between cycles. The resulting homogenate was carefully transferred to a 1.5 ml reaction tube and centrifuged at 17000 g, 4°C for 10 min using a bench-top centrifuge (Eppendorf). The supernatant was collected and stored at -80°C. Protein concentration in each lysate was determined using detergent-compatible protein assays (Bio-Rad). Subsequently, samples were mixed with a commercial 2x Tris-tricine sample buffer, with or without 0.05 M DTT, and an equal amount of protein to generate a series of probes with uniform protein concentration (4  $\mu\text{g}/\mu\text{l}$ ) for ensuing immunoblotting experiments.

### Immunoblotting

For each working solution, 20  $\mu\text{l}$  were applied per lane on precast 10–20% Tris-tricine (for amyloidogenic processing) or 4–12% Tris-glycine (for ATeam) SDS–PAGE gradient gels (Novex). Electrophoresis was conducted at 120 V for 2 h. Protein transfer was carried out using the Bio-Rad wet-blotting system at 500 mA for 1 hour onto low-fluorescent Immobilon-FL membranes (0.45  $\mu\text{m}$  pore size, Merck) activated with 100% methanol. The blot transfer buffer consisted of 25 mM Tris, 190 mM glycine, and 20% methanol. After a brief rinse with distilled water, total protein levels for normalization were determined using Fastgreen stain on the blot. Washed membranes were immersed in 0.0005% Fastgreen FCF (Serva) in a wash solution containing 30% methanol and 7% glacial acetic acid in distilled water for 5 minutes. Following two 1-min washes in the wash solution, membranes were visualized using a ChemoStar fluorescent imager (Intas). Subsequently, membranes were thoroughly washed in TBS with Tween (TBS-T, 0.05%) at least three times for 10 min each. Membranes were then blocked in 5% BSA in TBS-T at room temperature for 1 hour before overnight incubation in primary antibody solutions containing 5% BSA in TBS-T at 4°C on a rotating shaker. The primary antibodies used were: anti-C-terminus APP (rabbit, 127-005, Synaptic Systems, 1:500); anti-C-terminus human APP (mouse, 6E10, BioLegends, 1:1000); anti-N-terminus human APP (rat, 1D1, Merck, 1:500); anti-BACE1-3D5<sup>38</sup> (mouse, hybridoma culture supernatant, 1:500); anti-GFP (chicken, GFP-1010, Aves Labs, 1:1000). The next day, membranes were washed in TBS-T three times for 10 min each before incubation in secondary antibody solutions also containing 5% BSA in TBS-T. The secondary antibodies used were: anti-rabbit IgG Alexa 488 (Thermo-Fisher, 1:5000); anti-mouse horseradish peroxidase (HRP, Dianova, 1:10000), anti-rabbit HRP (Dianova, 1:10000), anti-rat HRP (Dianova, 1:10000), anti-chicken HRP (Dianova, 1:10000). After three 10-min washes in TBS-T, membranes were chemiluminescently scanned using the ChemoStar fluorescent imager (Intas). Prior to imaging, an equal amount of Western Lightning Plus ECL Oxidizing Reagent Plus and Enhanced Luminol Reagent Plus (PerkinElmer) were first mixed and then applied onto to the membrane. To visualize proteins with low abundance, SuperSignal West Femto Stable Peroxide and Luminol/Enhancer (Thermo) were instead utilized. For quantification based on raw images, background subtraction and band analysis were performed using Fiji<sup>40</sup> (integrated density). As immunoblotting was performed using samples from both sexes of experimental animals, normalization was performed using sex-specific controls. Target protein content was normalized to the Fastgreen bands of the respective controls as indicated in the graphs, along with the performed statistical analysis.

### Data analysis, statistics, and figure preparation

No animals or data points were excluded for this study. No statistical methods were used to pre-determine sample sizes but sample sizes for quantitative LSM are comparable to those shown in our past publication.<sup>3</sup> Specifically for interaction data in [Data S2](#), we ran separate analyses in R (version 4.3.2, R Core Team) for each pairing of region of interest—alveus, isocortex, hippocampus—and dependent measures—plaque volume, total plaque volume, and plaque density, plaque number. For average plaque volume, total plaque volume, and plaque density, we ran ANOVAs (Type III), with two factors (parent generation, grandparent generation), using `aov_ez` from the `afex` package.<sup>39</sup> For plaque number, we instead fit a Poisson regression (including, as before, the factors parent generation, grandparent generation, and their interaction (`glm`, family = “poisson”). Since all these models involve 2 x 2 comparisons, no post-hoc analyses are necessary. Aside from the aforementioned analysis, remaining statistical analyses and initial graphs were prepared using Prism 8.0.2 (GraphPad). Statistical tests were chosen based on tests for normality. Experimenters were blinded in the

transgenic inheritance pattern image analysis. Details of the specific analyses conducted are provided in the corresponding figure legends. Figures were created using Adobe Illustrator 29.0 (Adobe).

### Systematic review of 5xFAD studies

We performed a literature review of published studies that used the 5xFAD mouse line over the last five years (2019–2024) on the 9<sup>th</sup> of October 2024. Using the PubMed database, searching for “5xFAD” in titles and/or abstracts generated a total of 991 hits, with the 5-year publication date, English language, and excluding preprints criteria applied. To distinguish publications that were unfit for our literature review, the following filters were used: bibliography, biography, books and documents, collected work, comment, congress, dictionary, directory, editorial, expression of concern, guideline, interview, lecture, legal case, legislation, systematic review, news, newspaper article, personal narrative, practice guideline, preprint, retracted publication, review, scientific integrity review, systematic review, video-audio media, webcast. This resulted in 31 items to exclude from the initial list. Both lists were then uploaded to EPPI Reviewer, using the “mark duplicates” and “include/exclude” functions to remove as necessary. Through manually reviewing the 960 papers, we removed an additional 34 publications—ranging from reviews and retracted papers not caught by the initial filters, to studies that used published 5xFAD datasets but did not conduct experimental work using the model themselves. Four studies that bred 5xFAD mice homozygously were also excluded.

For the final tally of 922 studies, two researchers independently evaluated the papers based on the following parameters: whether the 5xFAD line was crossbred to another model; the background strain of 5xFAD mice used; sex of experimental animals used; reporting of breeding schemes (i.e., inheritance pattern) and the source of the 5xFAD transgene if reported. When papers cited other references for their husbandry and generation of experimental models, we also considered any additional information provided by the cited studies for the said parameters.

First, we took note of the background strains of the experimental models used in each study. The congenic C57BL/6 (B6) strain was indicated by B6.Cg-Tg(APPswF1on,PSEN1\*M146L\*L286V)6799Vas/Mmjax, #034848 or #008730 JAX strain numbers, while B6SJL-Tg(APPswF1on,PSEN1\*M146L\*L286V)6799Vas/Mmjax, #034840 or #006554 referred to the mixed C57BL/6 x SJL (SJL) strain. Studies were counted under a separate category under the congenic umbrella if they did not report the number of generations of backcrossing between SJL and B6 mice, while at least five generations of backcrossing was required for assigning to the full B6 category. Likewise, papers that only reported the strain of their wildtype controls were marked as such, given that we found instances where researchers used 5xFAD on the SJL background and B6 controls or vice versa, and thus could not reliably conclude that the 5xFAD mice were on the same background as their controls except where explicitly mentioned. In cases where 5xFAD mice were crossed with another model, we also checked the background strain of that model and classified these studies according to the criteria above.

Studies were also categorized according to whether they used female mice only, males only, both, or did not report the sex of the experimental animals at all. We then counted papers that pooled data from both male and female mice for their analyses regardless of the reasons stated, i.e., even when no significant differences were found between sexes or when male and female samples were marked by different symbols but were still averaged together for the same parameters. Meanwhile, cases where research groups compared sex effects; investigated the effects of a genotype or intervention in a sex-specific manner, thereby showing separate results for both male and female cohorts; and/or simply reported “sex-matched” in their analyses, even without specifying the sex of animals used per experiment—were all flagged as using “both sexes but separated analysis”. If papers pooled data for certain experiments but not others, we gave precedence to parameters reported to be most strongly affected by sex dimorphism in this model, such as amyloid plaque burden, gliosis, and/or behavior.

Lastly and most importantly to the present study, we checked whether studies detailed their breeding setups and the parental origin of the 5xFAD transgene as paternal or maternal inheritance. Cases wherein 5xFAD mice were obtained directly from The Jackson Laboratory (JAX) or the Mutant Mouse Resource and Research Center (MMRRC), with the authors citing either JAX/MMRRC or the relevant strain numbers, were marked separately as “using mice directly from JAX” and “likely following paternal inheritance”. Alternatively, we classified studies as non-inheritance reporting if 5xFAD mice were obtained from JAX, but in-house colonies were set up without mention of the sex of transgene-carrying breeders or if these mice were then crossbred to another line. Moreover, if 5xFAD mice were crossed with another model, and the inheritance pattern was cited for the initial 5xFAD colony but not for the subsequent crossbreeding, this was also marked as “no inheritance reported”. Importantly, we made a point to distinguish papers that did not report transgene inheritance and/or sex of the experimental animals, without assuming that research groups used both, as opposed to cases where the authors explicitly stated using both male and female 5xFAD breeders.

### Reporting of Thy1 promoter-driven transgenic AD models

We accessed the publicly available research model database on Alzforum (<https://www.alzforum.org/research-models>) to obtain information on transgenic AD models potentially affected by our experimental findings, specifically models using the Thy1 promoter to drive transgene expression. The search was performed on the 6<sup>th</sup> of November 2024 with the keyword “Thy1” and inclusion criteria of “Mouse” and “Alzheimer’s disease”. A total of 45 models were obtained, 5 of which were excluded due to these being *Trem2* cross-breeds with overlapping models of amyloidosis. The name, genetic background, modification details, transgene, and primary paper were reported in the “Thy1 AD models” tab of [Data S2](#).